SELF-HEALING CFRP FOR AEROSPACE APPLICATIONS

Dr Ian P Bond, Mr Gareth J Williams & Dr Richard S Trask
Advanced Composites Centre for Inovation and Science, University of Bristol, Department of Aerospace Engineering, Bristol, BS8 1TR, UK.
Email: I.P.Bond@bristol.ac.uk

Keywords: *multifunctional, self-healing, repair, damage tolerance, fracture*

Abstract

The planar nature of a FRP structure results in relatively poor performance under impact loading. Furthermore, significant degradation in material performance can be experienced with minimal visual indication of damage, a scenario termed Barely Visible Impact Damage (BVID). Current damage tolerant design philosophies incorporate large margins to account for reduction in performance due to impact events, resulting in overweight and inefficient structures. An alternative approach to mitigate impact damage sensitivity can be achieved by imparting an ability to undergo self-healing. Self-healing composites would allow lighter, more efficient structures and would also offer a potentially substantive reduction in maintenance and inspection schedules and their associated costs. This paper considers the development of autonomic self-healing within CFRP, and demonstrates the strength recovery possible when a resin filled hollow fibre is distributed at specific interfaces within a laminate, minimizing the reduction in mechanical properties whilst maximizing the efficiency of the healing event.

1. Introduction

The development of advanced fibre reinforced polymer's (FRP's) to achieve performance improvements in engineering structures focuses on the exploitation of the excellent specific strength and stiffness that they offer. Recently, research has focused on taking advantage of their hierarchical microstructure to facilitate the incorporation of additional functionality giving further benefit to their use over metallic rivals. However, the planar nature of an FRP's microstructure results in relatively poor performance under impact loading. Furthermore, significant degradation in material performance can be experienced with minimal visual indication of damage being present, a design scenario termed Barely Visible Impact Damage (BVID). Current damage tolerant design philosophies incorporate large margins to account for reduction in structural performance due to impact events, resulting in overweight and inefficient structures. An alternative approach to mitigate impact damage sensitivity can be achieved by imparting the ability for these materials to undergo self-healing thereby reducing the importance of detecting and alleviating damage. Self-healing composites would allow lighter, more efficient structures which would have a significant influence in addressing environmental concerns regarding aviation and would also offer a potentially substantive reduction in maintenance and inspection schedules and their associated costs.

Naturally occurring 'materials' have evolved into highly sophisticated, integrated, hierarchical structures that commonly exhibit multifunctional behavior [1]. Inspiration and mimicry of these microstructures and micro-mechanisms offer considerable potential in the design and improvement of material performance [2] Many of the biological processes involved are extremely complex. Bio-inspired self-healing takes inspiration from biological repair systems, however, it necessarily assumes a more simplified approach.

Applications for self-healing have been considered in bulk concrete [3-5], bulk polymers [6] and polymer composites [7-10]. In particular, self-healing for polymer composites has seen significant developments in recent years [11-22] using the inspiration of biological self-healing applied with broadly traditional engineering approaches. Self-healing in polymer composites can be divided into two fundamental design paths, of which this paper considers the latter:

1) Modification of the matrix material to contain a healing agent or facilitate healing [6,9,11]
2) Inclusion of storage vessels containing a healing agent within the material [12-22].

The storage vessel of choice for this study is hollow glass fibre (HGF) [23,24] which is used in preference to microcapsules [25,26] because they offer the advantage of being able to store a significant volume of functional agents for self-repair, as well as allowing easy integration with the surrounding reinforcement. A bespoke HGF manufacturing facility [23,24] has been used to produce fibres between 30μm and 100μm diameter with a hollowness of approximately 50%. These are embedded within either glass fibre-reinforced plastic (GFRP) or carbon fibre-reinforced plastic (CFRP) and infused with uncured resin to impart a self-healing functionality to a laminate. During a damage event some of these resin filled fibres rupture, releasing the stored healing agent into a damage site, thus initiating the recovery of properties (healing). This ameliorates critical effects of matrix cracking and delamination and most importantly prevents further damage propagation.

The precise details of the healing agent can take several forms suitable for containment within HGF [10]: a one-part system, a two-part resin and hardener system, or a resin system with a catalyst or hardener. The exact nature of the self-healing method to be deployed depends upon (i) the nature and location of the damage, (ii) the choice of repair resin, and (iii) the influence of the operational environment. The HGFs can be introduced within a laminate as additional plies [18-20] at each interface, at damage critical interfaces or as individual filaments spaced at predetermined distances within each ply [21,22].

This paper considers the development of autonomic self-healing within CFRP, and demonstrates the strength recovery possible when a resin filled HGF system is distributed at interfaces within a laminate, minimizing the reduction in mechanical properties whilst maximizing the efficiency of the healing event. In order to more fully understand and optimize the healing process, two studies were conducted for CFRP systems considering the following properties of the laminates:

1) Flexural four point bend: *Assessment of flexural strength of CFRP damaged by quasi-static indentation*
2) Compression after impact: *Assessment of compressive strength of CFRP damaged by drop weight impact*

a) Mechanical performance: *Undamaged, assess disruption caused by embedded HGF*
b) Damage Tolerance: *Damaged, assess interaction between HGF and impact damage*
c) Healing Potential: *Damaged + Healed, assess healing efficiency*

2. Flexural Strength Analysis

Four point bend flexural testing (ASTM D6272-02) [27] was initially used to assess laminate performance as it is a simple, reliable test which has been successfully used to demonstrate self-healing in GFRP [18-20]. Furthermore, quasi-static indentation can be considered analogous to low velocity impact events [28] and so it was deemed to be suitable for the generation of damage representative of that from a low velocity impact event.

2.1. Manufacture

Carbon fibre/epoxy (Hexcel T300/914) pre-impregnated tape was selected to manufacture the host laminate as it is used in a variety of aerospace applications. Quasi-isotropic (QI) plates (230mm x 160mm x 2.6mm) were manufactured using hand lay-up [16 ply (-45°/90°/45°/0°)2S]. Cure was undertaken according to manufacturer's recommendations. Two different HGF distributions with fibre pitch spacing of 70μm and 200μm were wound directly onto uncured CFRP plies prior to lamination. The HGF had an external diameter of 60μm and an internal bore of 42μm, to provide a hollowness fraction of 50%. These variations in HGF spacing were to allow an investigation of the fundamental trade-off between supplying an appropriate volume of healing resin and minimizing the disruption caused by the HGF on the host laminate. The 70μm pitch ensured that the fibres were effectively immediately adjacent to each other, and the 200μm spacing ensured approximately three fibre diameters spacing between HGF so that optimal embedment was achieved within the laminate. HGF was located at two 0º/-45º interfaces within the lay-up as follows and in the same orientation as the 0º ply:

(-45°/90°/45°/0°/**HGF**/-45°/90°/45°/0°/
0°/45°/90°/-45°/**HGF**/0°/45°/90°/-45°)

This interface was selected as the location for HGF embedment to fulfill two requirements:

1) The 0° direction (i.e. the longest dimension of the test samples) ensured that a maximum length of HGF was contained within the sample and consequently a maximum amount of healing resin was available.
2) Previous work [29-31] regarding the embedment of optical fibre within a composite, states that an optimum is achieved when the embedded fibre possesses the same orientation of at least one of the adjacent plies.

Although the 0° ply direction is significant in terms of providing the load bearing capability of the laminate, for these high aspect ratio samples it was essential to maximize the potential volume of healing resin supplied per HGF fracture. The two HGF distributions resulted in either 3% or 1% HGF volume fractions within each test specimen, which were capable of storing 197 mm^3 and 69 mm^3 healing resin respectively.

2.2 Testing

A support span to depth ratio of 32:1 and a support span to load span ratio of 3:1 were selected according to ASTM D6272-02. This resulted in specimen dimensions of 100mm x 20mm x 2.6mm. Each sample was measured and average values were used for strength calculations in accordance with the ASTM standard. The variation in thickness between samples was less than 1.5%. Ten samples were cut from a plate with the use of a water-cooled diamond grit saw. The sample edges were polished with SiC paper (P2500) to avoid any unwanted edge effects. Samples were then dried, sealed in sample bags and stored in a temperature and humidity controlled environment prior to testing. Immediately prior to mechanical testing, the HGF within each specimen were infiltrated with a healing agent of pre-mixed, two-part epoxy resin (Cytec Cycom 823) with mix ratio 4:1 by weight using a vacuum assist technique.

Quasi-static impact damage was imparted to each specimen using a 5mm diameter spherical tup mounted on a Hounsfield H20K-W (20kN load cell) electromechanical test machine under load control. The sample was supported by a steel ring of 27mm outer diameter and 14mm inner diameter. The indentations were stopped at a peak load of 2000N. Up to this load level the damage is contained within the laminate and can be likened to BVID: surface indent <0.3mm), minimal back face distortion/fibre break-out. Furthermore, the shear crack/delamination distribution within the laminate forms the characteristic ‘pine tree’ distribution as would be expected from a low velocity drop weight impact event.

After indentation, the specimens were left at 70ºC for 45 minutes to reduce healing resin viscosity (25cps) and facilitate infiltration into damage sites. This was followed by a cure schedule of 125ºC for 75 minutes. Whilst this process diverges from the original aim of achieving an autonomic healing ability, the use of a pre-mixed healing resin and elevated temperature after a damage event allowed the Cycom 823 to reach an optimum cure status meet and for the study to demonstrate the highest level of healing efficiency possible with this system. Cycom 823 is not designated a ‘healing agent’ and was chosen as the best available commercial system to fulfill this role. In fact, no epoxy resin system is currently available which is specifically designed for such an application (i.e. low viscosity, insensitivity to mix ratio, rapid cure under ambient conditions and prolonged shelf life). However, one practical advantage of using such a resin system for the demonstration phase of this study is that temperature activation provides excellent control of cure initiation, eliminating time constraints on the testing/manufacturing process.

After healing, test specimens were mounted on a Roell Amsler HCT25 electro-mechanical test machine with roller spacing determined by specimen dimensions and ASTM D6272-02. An Instron 8800 controller/data-logger was used to control the test machine and record data. Specimens were loaded to catastrophic failure at which point the cross-head was stopped and the load removed. Specimens were monitored to ensure a consistent failure mode and optical microscopy used to record detailed observations. Results were obtained from ten undamaged, five damaged and five healed specimens.

2.3 Microscopy

Microscopic characterization of the CFRP laminates with embedded HGF gives an insight into the possible effects of their presence. This is a useful tool, and will be used in conjunction with mechanical results to understand the impact behavior of the laminates. Figure 1 shows the distribution of HGF when spaced at 70µm within the laminate and how they are spaced ideally (b) side by side, however low

tackiness of the matrix resin during manufacture leads to HGF clumping (c) as they detach and reattach at overlapping positions during the hand lay-up process generating resin rich regions.

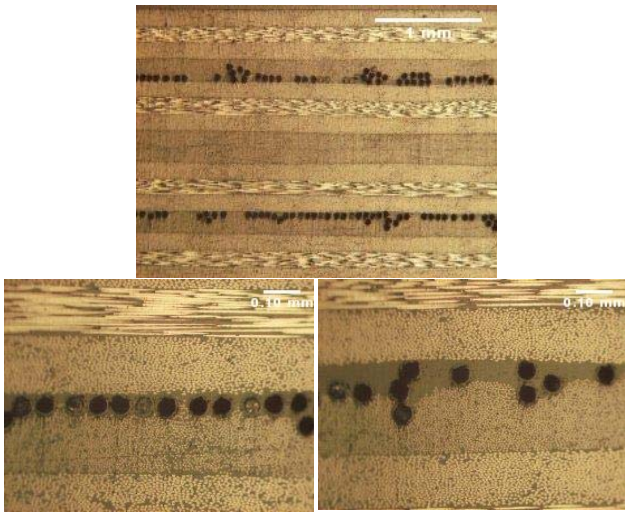

Fig. 1. (top) 70µm spaced HGF with (left) good embedment (right) HGF clumping.

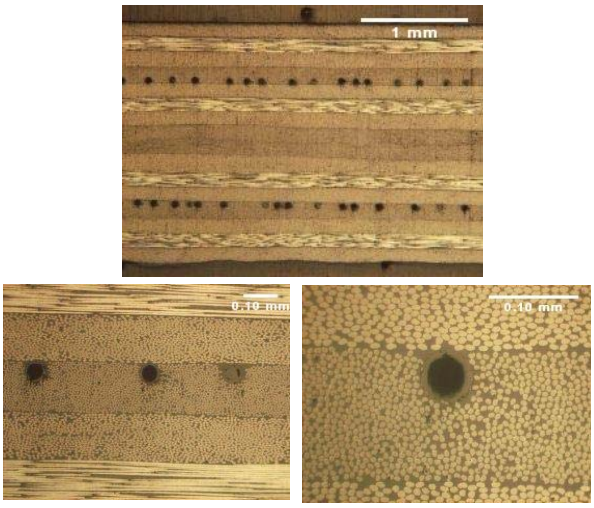

Fig. 2. (top) 200µm spaced HGF at two interfaces (left) showing consistent spacing and (right) ideally embedded.

Figure 2 shows the distribution of HGF when they are spaced at 200µm (a). The consistency of their positioning is improved and are ideally spaced at three HGF diameters (b) allowing them to embed with minimal disruption to the laminate (c).

2.4 Results

The results of the four point bend flexural testing are shown in Table 1. Comparisons are made between the performance of undamaged, damaged and healed specimens for the two HGF pitch spacings alongside a baseline CFRP laminate with no HGF. The results show that at low HGF spacing (70µm) a small reduction (8%) in flexural strength is incurred by their inclusion which is attributed to the resin rich regions and disruptions to the laminate generated by HGF clumping, shown in Figure 1c. However, this configuration can also be seen to exhibit a degree of increased damage tolerance (i.e. higher residual strength after damage) compared to both the higher pitch spacing HGF and the baseline laminate. This is primarily attributed to HGF 'crushing' and fracture as propagating crack fronts rupture HGF. The detrimental effects of HGF inclusion are outweighed by the strength recovery achieved by a healing event which recovers 97% of the laminates undamaged strength. This suggests that the increase in healing resin storage volume provided by higher HGF volume fraction is beneficial for the recovery of mechanical properties and combined with an increase in damage tolerance, mitigates the initial reduction in mechanical performance of the undamaged state.

Table 1. Effect of HGF and Healing on Flexural Strength of CFRP.

Specimen type		**Undamaged (CV%)**	**Damaged (CV%)**	**Healed (CV%)**
Plain CFRP	Flexural strength (MPa)	583.3 (2.3)	405.0 (16.2)	-
	% of undamaged baseline	*100%*	*69%*	-
HGF spaced @70µm	Flexural strength (MPa)	534.9 (2.4)	443.7 (10.7)	519.6 (5.5)
	% of undamaged baseline	*92%*	*76%*	*89%*
HGF spaced @200µm	Flexural strength (MPa)	568.8 (3.3)	401.0 (13.2)	466.6 (4.7)
	% of undamaged baseline	*98%*	*69%*	*80%*

3. Compression After Impact Analysis

Compression after impact provides a rigorous assessment of a material performance following an impact damage event. The material compressive strength is extremely sensitive to internal damage and provides a critical assessment of self-healing efficacy. Furthermore, drop weight impact is an industry standard for recreating low velocity impact damage typically found in an operational environment. Testing was conducted in close accordance with ASTM D7137/D7137M-05 [32], but with modifications in accordance with the test method proposed by Prichard and Hogg [33]. This allows for smaller coupon sizes allowing some continuity for the laminate design previously used in the four point bend flexural strength studies.

3.1 Manufacture

Again, carbon fibre/epoxy (Hexcel T300/914) pre-impregnated tape was selected for manufacture of the host laminate. Quasi-isotropic (QI) plates (210mm x 210mm x 2.6mm) were manufactured using hand lay-up [16 ply (-45°/90°/45°/0°)2S]. Cure was undertaken according to manufacturer's recommendations. Three different HGF distributions of fibre pitch spacing 70µm, 140µm and 200µm were wound directly onto uncured CFRP plies prior to lamination. The HGF had an external diameter of 60µm and an internal bore of 42µm, to provide a hollowness fraction of 50%. The HGF was located at an increased number of interfaces in order to increase the volume of healing resin stored, and to increase the through thickness distribution of its supply. This was necessary as the low velocity drop weight impact created a larger damage region within the laminate than that produced with quasi-static indentation, due to the increase in tup diameter and support ring providing the boundary conditions. HGF was located at either two or four 0º/45º interfaces within the lay-up as follows and in the same orientation as the 0º ply:

(-45°/90°/45°/0°/**HGF**/-45°/90°/45°/0°/
0°/45°/90°/-45°/**HGF**/0°/45°/90°/-45°)

1) 70µm: HGF adjacent fibres, high HGF content, high disruption (*3% Vf, 197mm^3 storage volume*)
2) 140µm: 2x HGF diameter spacing, medium HGF content, medium disruption (*2% Vf, 99mm^3 storage volume*)
3) 200µm: 3x HGF diameter spacing, low HGF content, low disruption (*1% Vf, 69mm^3 storage volume*)

(-45°/90°/45°/**HGF**/0°/**HGF**/-45°/90°/45°/0°/
0°/45°/90°/-45°/**HGF**/0°/**HGF**/45°/90°/-45°)

4) 200µm: 3x HGF diameter spacing, medium HGF content, medium disruption (*2% Vf, 138mm^3 storage volume*)

Initial testing was conducted on specimens containing either 70µm, 140µm, 200µm or 200µm at 4 interfaces, all with impact energies of 6J. However, is was discovered that the brittle nature of the non-toughened 914 epoxy resin matrix combined with the impact boundary conditions resulted in damage saturation of the laminates with significant back face damage. Furthermore, ultrasonic 'time-of-flight' C-scans showed that beyond 4J impact energy, the damage distribution diverged from the characteristic pine-tree profile as the upper face sub-laminate delaminations extended to the same profile areas as the lower region which were effectively 'pinned' by the boundary conditions preventing further propagation and causing significant back-face breakout. This meant that the damage could no longer be realistically considered as BVID. Moreover, it became apparent that these configurations could not provide sufficient healing resin volume for the damage volume generated. Also, locating HGF at just two interfaces relied heavily upon adequate connectivity within the damage network to distribute the healing resin. Therefore, a more optimized design was considered whereby two different HGF distributions were located at five different interfaces within the laminate, as shown below. HGF with 140µm pitch spacing were located at two interfaces above the centre line, and HGF with pitch spacing of 70µm were located at three interfaces below the centerline. This was in order to provide significant healing resin volume at close proximity to the larger delaminations typically created nearer the back face whilst also providing sufficient healing resin to address the less significant damage towards the upper surface:

(-45°/90°/45°/**HGF**$_{70}$/0°/**HGF**$_{70}$/45°/
90°/45°/**HGF**70/0°/0°/**HGF**(140)/45°/
90°/-45°/0°/**HGF**(140)/45°/90°/-45°)

5) 70µm & 140µm: Very high HGF content, location weighted towards back face where larger delaminations expected (*6% Vf, 394mm3 storage volume*)

3.2 Testing

An instrumented impact tester (Instron Dynatup 9250HV) was used to generate low velocity impact damage. The impact boundary conditions were determined by guidelines proposed by Prichard and Hogg [33] which determines test conditions in close accordance with other published test methods for impact and CAI such as ASTM [32]. However, they propose modifications to allow smaller, thinner laminates to be tested (<3mm). An energy level of 3J was selected for impact events, by assessing the response of the laminate to a range of energy levels (1J negligible damage - 6J significant back face break out). A hemispherical tup of radius 20mm and impactor mass of 5.27kg struck laminates clamped between two 10mm steel plates with a circular impact window of 40mm diameter. Four hand-tightened M16 bolts generated the clamping force between the two steel plates. Immediately after impact, laminates were again subject to a healing cycle by being placed in an oven at 70ºC for 45 minutes to reduce healing resin viscosity (to 25cps) and facilitate infiltration into damage sites. This was followed by a cure schedule of 125ºC for 75 minutes. Again, this deviation from autonomic self-healing is justified by a desire to establish the most effective healing possible. The pre-mixed Cycom 823 resin system will cure in 7 days at ambient temperature which could improve healing via reduced thermal mismatches during cure and an increased time period for infiltration of the damage. However, a controlled and defined healing cycle of less than two hours was deemed more practical for this study.

CAI testing was conducted using an Instron 1342 with a 250kN load cell and an Instron 8800 controller/data-logger was used to control the test machine and record the data. Samples were loaded into a test rig based on the ASTM standard [30] and modified in accordance with Prichard and Hogg to allow 6 samples of 89mm x 55mm x 2.6mm to be tested. Samples were loaded at a rate of 0.4mm/min until failure at which point the crosshead was stopped. The specimen was then unloaded and removed. Strain measurements were made using a full field train measurement technique on the front face of the specimens in order to monitor any deformation and/or buckling.

3.3 Results

Table 2. Effect of HGF content and healing on CAI strength of CFRP

Specimen type		Undamaged (CV%)	Damaged (CV%)	Healed (CV%)
Plain CFRP	Strength (MPa)	343.98	-	-
	% of undamaged baseline	*100%*	-	-
HGF @5 interfaces	Strength (MPa)	348.52	217.99	315.30
	% of undamaged baseline	*101%*	*63%*	*92%*

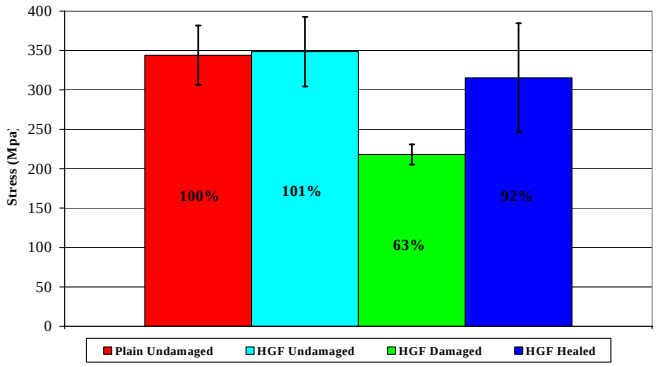

Fig. 3. Comparison of compression after impact strength for plain baseline laminate and self-healing CFRP.

The results from CAI testing are shown in Table 2 and Figure 3. Table 2 shows that under compressive loading there was no apparent reduction in failure stress due to the presence of HGF, regardless of the visible disruption to the laminates that is evident in Figure 4a. The majority of this disruption was due to the un-optimized manufacturing process and could be improved to achieve the ideal HGF distributions that can be seen in Figures 4b and 4c. This may be due to the failure mode of the undamaged samples being more sensitive to the boundary conditions of the testing rig. Any fluctuations in laminate thickness or clamping force of the supports could initiate a failure at high loads. However, that is not to say that the presence of HGF in the laminates would cause a

reduction in the failure stress under compression. HGF are inherently stable in compression as they have a high second moment of area, furthermore the compressive load would be carried by the reinforcing carbon fibres. Therefore, the only feasible reduction in compressive strength would be due to a reduction in carbon fibre in the 0°, however locating the HGF at any other angle may cause waviness in the 0° which could be more problematic by inducing buckling. Currently, any waviness in the laminates is in the transverse direction due to variations in ply thickness caused by HGF which has no affect on the longitudinal buckling properties. Furthermore, there is no evidence that carbon fibre volume fraction is reduced in preference to a reduction in the matrix resin or an increase in laminate thickness: the average thickness of laminates with HGF is 0.1mm thicker than the plain laminate. Other disruptions can be caused by resin rich regions generated by HGF clumping, however this can be eradicated by refinement of the manufacturing process, and is also dependent on the tackiness of the host laminate pre-preg in order to hold the HGF in place during manufacture.

It can also be seen that after laminates were damaged and healed, they recovered on average 92% of their undamaged strength. Figure 3 portrays the scatter present at each stage of testing. It is evident that the undamaged samples experience a large variation in failure stress, this is due to the sensitivity of the failure on clamping boundary conditions therefore any fluctuations in laminate thickness or dimensions can reduce/increase the effectiveness of the boundary conditions thereby affecting the load at which failure occurs. The damaged samples exhibit significantly reduced fluctuations in failure stress as impact damaged laminates are very sensitive to compressive loading as delaminations are propagated causing formation of sub-laminates, instability and ultimately leading to buckling failure. Healed samples exhibit the largest fluctuations in failure strength, this is largely due to two samples which exhibited limited healing and are considered later.

3.4 Microscopy and Damage Analysis

Microscopic characterization of the CFRP laminates containing embedded HGF provides an insight into the effect of the HGF configurations on laminate response to impact and their subsequent mechanical behavior. Scanning electron microscopy (SEM) was also used to provide further insight into the interaction between HGF and damage within the laminate. Figure 4 shows the distribution of HGF within the laminate, at spacings of 70µm and 140µm HGF.

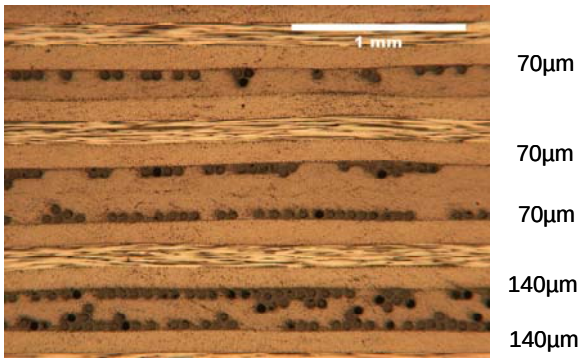

Fig. 4. HGF at five interfaces showing overall HGF distribution.

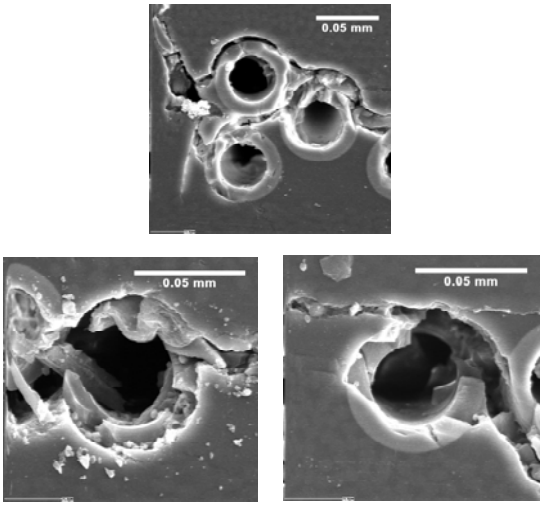

Fig. 5. SEM micrographs: (top) delamination crack energy dissipated as it passes around HGF, (lower left) crack passing directly through HGF (lower right) crack passing around and through cluster of HGF.

Figure 5 shows the interaction between HGF and propagating crack fronts within CFRP due to impact damage. Figure 5 (top) shows a reduction in crack opening displacement after passing though a single HGF. This suggests that some of the propagation energy is used to initiate fibre rupture and correlates with the findings in Table 1 where laminates containing HGF were observed to have higher post-impact residual strengths compared to

plain laminates. Figure 5 (lower left) shows how a propagating crack has shattered a single HGF and illustrates the significant energy that must be expended in this process. Finally, Figure 5 (lower right) shows a crack intercepting a cluster of HGF at which point it divides into both interfacial cracks around HGF combined with fibre rupture. The rupture of HGF not only provides an additional mechanism for energy absorption but is critical to the function of this self-healing approach.

Ultrasonic C-scanning is a powerful non-destructive test (NDT) method which is used here to investigate the damage distribution within the laminates and also to compare their compressive failure modes. In particular, 'time of flight' analysis (TOF) is extremely useful for investigating impact damaged samples as it allows differentiation between delaminations at different ply levels through the thickness of the laminate. However, delaminations towards the surface have a 'shading' effect on damage below, therefore scans are taken looking at the front and back face of the laminates in order to look in detail at all delaminations present within the laminate.

Coupons that were damaged at 3J impact energy consistently failed between 60% and 70% of the undamaged failure stress by a process of localized buckling at the mid-section. This is illustrated in Figure 6 (lower) where delaminations extend across the width of the specimens. Coupons that were healed after 3J impact were able to sustain loads up to and exceeding the undamaged failure stress. However, there was a significant degree of scatter in the results (Table 2) as two of the coupons showed only a limited degree of strength recovery. This is confirmed in Figure 6 (upper) where coupons 1, 3 and 5 failed due to compressive buckling at the mid-section, whereas coupons 2 and 4 failed by end brooming (the same failure mode as exhibited by undamaged coupons). However, although coupon 3 failed by localized buckling in the mid-section, it sustained 90% of the undamaged laminate failure stress, thus still exhibiting a significant degree of healing. It is evident upon comparison of images in Figures 6 that healed coupons 1, 3 and 5 typically have a significantly larger delamination area after failure than the equivalent damaged samples, this may be indicative that the healing agent was able to prevent the initial propagation of delaminations up to a critical load threshold, at which point the healing resin failed leading to rapid delamination propagation and hence catastrophic buckling failure. This may have been due to incomplete infiltration of the healing resin into the damage area or a weak bond between healing resin and parent matrix.

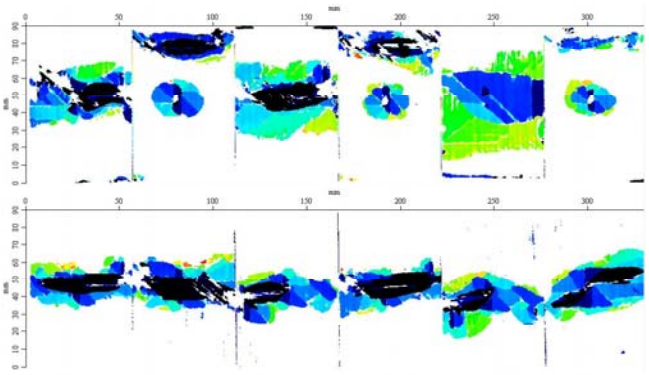

Fig. 6. Ultrasonic TOF of failed samples (1-6, left to right) after CAI testing, (upper) healed (lower) damaged.

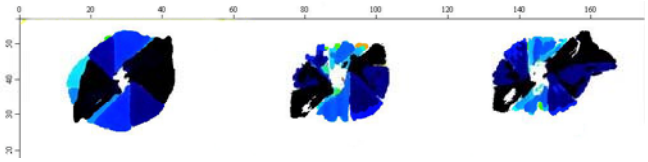

Fig. 7. Ultrasonic TOF at the back face of (left) damaged laminate, (centre & right) damaged and healed.

Figure 7 (left) shows a C-scan TOF image of an impacted (3J) coupon (before CAI testing) which exhibits the classic 'peanut' shape delaminations at different through thickness interfaces within the laminate (indicated by the different shades). Figure 7 (centre and right) also shows C-scan TOF images of coupons damaged by similar 3J impacts which have been subsequently failed by CAI testing. It can be seen at the markers indicated 1 and 2, that the delaminations have been reduced in size in comparison with Figure 7 (left). Furthermore, the edges of the delaminations are no longer clearly defined. This is indicative that these crack tips have been infiltrated with healing resin and have been blunted sufficiently to prevent the delaminations propagating when loaded in compression. Further investigations are ongoing to establish the exact form of healing resin infiltration away from the crack tip.

The process of self-healing invariably relies upon the occurrence of HGF fracture initiated by a damage event and connectivity between HGF and the subsequent damage network generated within laminate. Therefore, the location of the HGF within a laminate is expected to have a significant effect on healing efficiency. In this study, the embedment of HGF was optimized in order to reduce disruption to the laminate, and to provide the maximum length of individual HGF in order to maximize the volume of resin available per HGF fracture. The latter condition was determined by the specimen sample size and would be different for real structural applications. In reality, the manufacturing method employed for HGF would allow the orientation of HGF at any desired angle to match any interface at which it was required. Furthermore, as the 0° reinforcing fibres are the primary load bearing fibre for in plane forces, it may be beneficial to locate the HGF at a different interface in order to minimize the degradation to the mechanical performance of the laminate.

4. Conclusions

This work has conclusively proven that embedded resin filled hollow glass fibres impart a capability for CFRP laminates to self-heal after low velocity impact damage. It has also demonstrated the excellent potential offered by self-healing without significant detrimental effect on the host laminate. In fact, the presence of HGF is seen to increase the damage tolerance of the material. This has been demonstrated in four point bend flexural testing after quasi-static impact and in compression after drop weight impact, where strength recovery after healing in both cases exceeded 92%.

The flexural analysis showed that the initial reduction in mechanical performance due to a low HGF spacing of 70µm was compensated by an increase in damage tolerance and a 97% strength recovery after healing. This initial reduction may possibly be improved by optimising the manufacturing to ensure better integration of HGF to avoid clumping and generation of resin rich regions.

CAI analysis combined with drop weight impact provided a much more stringent assessment of the laminates performance. However, compressive testing of the undamaged laminates appeared to be insensitive to the presence of HGF in contrats to the flexural testing. Ongoing work regarding self-healing for CFRP is studying the effects of using a toughened resin system as the host laminate, and testing of thicker laminates and larger coupon sizes in order accordance with the ASTM standard. Further work is needed to comprehensively characterize the interaction between the HGF, the stored healing resin and the formation of damage within the laminate.

Acknowledgments

The authors would like to acknowledge the UK Engineering and Physical Sciences Research Council for funding this research under Grant No. GR/TO3390 and Cytec Engineered Materials Ltd. for providing the Cycom 823 resin.

References

[1] Curtis, P. T. ”Multifunctional polymer composites”. *Advanced Performance Materials* Vol.3, No.3-4 1996, pp279–293.

[2] Kassner, M. E. et al. “New directions in mechanics” *Mechanics of Materials* Vol.37, 2005 pp231–259.

[3] Li, V. C., Lim, Y. M. and Chan, Y. W. “Feasibility of a passive smart self-healing cementitious composite” *Composites B* Vol. 29B, 1989, pp819–827

[4] Dry, C. “Matrix cracking repair and filling using active and passive modes for smart timed release of chemicals from fibres into cement matrices” *Smart Materials and Structures* Vol. 3, 1994, pp118–123.

[5] Dry, C. and McMillan, W. “Three-part methylmethacrylate adhesive system as an internal delivery system for smart responsive concrete” *Smart Materials and Structures* Vol.5, 1996, pp297–300.

[6] Chen, X., Dam, M. A., Ono, K., Mal, A. K., Shen, H., Nutt, S. R., Sheran, K. and Wudl, F. “A thermally re-mendable cross-linked polymeric material” *Science* Vol.295, 2002, pp1698–1702.

[7] Dry, C. “Procedures developed for self-repair of polymer matrix composites,” *Composite Structures* Vol.35, 1996, pp263–269.

[8] Motoku, M., Vaidya, U. K. and Janowski, G. M. “Parametric studies on self-repairing approaches for resin infused composites subjected to low velocity impact,” *Smart Materials and Structures* Vol. 8, 1999, pp623–638.

[9] Zako, M. & Takano, N. “Intelligent materials systems using epoxy particles to repair microcracks and delamination in GFRP,” *Journal of Intelligent Material Systems and Structures* Vol.10, 1999, pp836–841.

[10] Bleay, S.M., Loader, C.B., Hawyes, V.J., Humberstone, L. and Curtis, P. T. “A smart repair system for polymer matrix composites,” *Composites A* Vol.32, 2001, pp1767–1776.

[11] Hayes, S.A., Jones, F.R., Marshiya, K. and Zang, W. "A self-healing thermosetting composite material," *Composites A* Vol.38, 2006, pp1116-1120

[12] White, S. R., Sottos, N. R., Moore, J., Geubelle, P., Kessler, M., Brown, E., Suresh, S. and Viswanathan, S. Autonomic healing of polymer composites," *Nature* Vol.409, 2001 pp794–797.

[13] Kessler, M. R., White, S. R. and Sottos, N. R. "Self-healing structural composite materials," *Composites A* Vol.34, 2003 pp743–753.

[14] Brown, E.N., White, S.R. and Sottos, N.R. "Retardation and repair of fatigue cracks in a microcapsule toughened epoxy composite-part I: manual infiltration," *Composites.Science and.Technology* Vol.65, 2005a, pp2466–2473.

[15] Brown, E. N., White, S. R. and Sottos, N. R. "Retardation and repair of fatigue cracks in a microcapsule toughened epoxy composite-part 2: in situ self-healing. *Composites Science and Technology*," Vol.65, 2005b, pp2474-2480.

[16] Mauldin, T.C., Rule, J.D., Sottos, N.R., White, S.R. and Moore, J.S "Self-healing kinetics and the stereoisomers of dicyclopentadiene". *Journal of The Royal Society Interface*, Vol. 4, No. 13, 2007, pp.389-394.

[17] Jones, A.S., Rule, J.D., Moore, J.S., Sottos, N.R. and White, S.R. Life extension of self-healing polymers with rapidly growing fatigue cracks", *Journal of The Royal Society Interface*, Vol. 4, No. 13, 2007, pp.395-404.

[18] Pang, J. W. C. and Bond, I. P. "Bleeding composites-damage detection and self-repair using a biomimetic approach," *Composites A* Vol.36, 2005a, pp183–188.

[19] Pang, J. W. C. and Bond, I. P. "A hollow fibre reinforced polymer composite encompassing self-healing and enhanced damage visibility," *Composites Science and Technology* Vol.65, 2005b, pp1791–1799.

[20] Trask, R. S. & Bond, I. P. "Biomimetic self-healing of advanced composite structures using hollow glass fibres," *Smart Materials and Structures* Vol.15, 2006, pp704–710.

[21] Williams, G.J, Trask, R.S. and Bond, I.P, *Journal of The Royal Society Interface*, Vol. 4, No. 13, 2007, pp.363-372.

[22] Williams, G. W, Trask, R. S. and Bond, I. P, *Composites A*, Vol. 38, No. 6, 2007, pp.1525-1532.

[23] Hucker, M., Bond, I. P., Foreman, A. and Hudd, J. "Optimisation of hollow glass fibres and their composites," *Adv.anced Composites Letters* Vol.8, 1999, pp181–189.

[24] Hucker, M. J., Bond, I. P., Haq, S., Bleay, S. and Foreman, A. "Influence of manufacturing parameters on the tensile strengths of hollow and solid glass fibres," *Journal of Materials and Science* Vol.37, 2002, pp309–315.

[25] Brown, E. N., Kessler, M. R., Sottos, N. R. and White, S. R. In situ poly(urea formaldehyde) microencapsulation of dicyclopentadiene," *Journal of Microencapsulation* Vol.20, 2003, pp719–730.

[26] Rule, J. D., Brown, E. N., Sottos, N. R., White, S. R. and Moore, J. S. "Wax-protected catalyst microspheres for efficient self-healing materials," *Advanced Materials* Vol.17, 2005, pp205–208.

[27] Anon, Standard test method for flexural properties of unreinforced and reinforced plastics and electrical insulating materials by four-point bending. ASTM International, D 6272-02;

[28] Anon, Standard Test Method for Measuring Damage Resistance of Fibre-Reinforced Polymer-Matrix Composite to Concentrated Quasi-Static Indentation Force. ASTM International, D 6264

[29] Shivakumar, K. and Emmanwori, L "Mechanics of failure of composite laminates with an embedded fibre optic sensor," *Journal of Composite Materials* Vol.38, No.8, 2004, pp669-680

[30] Leka, L.G. and Bayo, E. "A close look at the mebedment of optical fibres into composite structures," *Journal of Composites Science and Technology* Vol.11, No.3, 1989, pp103-112

[31] Case, S.W. and Carman, G.P. "Compression strength of composites containing embedded sensors or actuators," *Journal of Intelligent Material Systems and Structures*, Vol.5, 1994, pp4-11

[32] Anon, Standard test method for compressive residual strength properties of damaged polymer matrix composite plates. ASTM International, D 7137/D 7137M-05

[33] Prichard, J.C. and Hogg, P.J. "The role of impact damage in post-impact compression testing," *Composites* Vol.21, No.6 1990, pp503-511